JOURNAL OF CATALYSIS 104, 424–433 (1987)

Temperature-Programmed Decomposition of Deuterated Formic Acid on Ni/SiO_2

JOHN L. FALCONER,[1] L. CRAIG BURGER, ISABELLE P. CORFA, AND KEVIN G. WILSON

Department of Chemical Engineering, Campus Box 424, University of Colorado, Boulder, Colorado 80309-0424

Received September 30, 1986; revised November 18, 1986

Decomposition of deuterated formic acid (DCOOH) was studied on supported Ni/SiO_2 catalysts at atmospheric pressure by using temperature-programmed decomposition (TPD) to allow a direct comparison to similar studies on single crystal nickel surfaces under ultrahigh vacuum. A bimolecular reaction mechanism appears to be occurring on both surfaces; the acid hydrogens form predominantly water while the carbon-bonded hydrogens form predominantly molecular hydrogen. The formation of D_2 and CO_2 is limited by decomposition of a surface intermediate and not by desorption. The formation of the CO product is limited by desorption, however, as was observed in single crystal studies. Though studies at atmospheric pressure on supported nickel are influenced by readsorption, CO disproportionation, adsorption on the support, and exchange reactions, agreement between the studies at vastly different pressures is quite good.

INTRODUCTION

Formic acid decomposition has been studied extensively on supported and unsupported metals, particularly nickel (*1–7*). Two reaction pathways are possible: dehydration and dehydrogenation. Based on kinetic and IR data, it appeared that decomposition proceeded through a formate intermediate (*5–7*). More recent temperature-programmed desorption (TPD) studies on clean, single crystal nickel surfaces under ultrahigh vacuum (*8–13*), however, indicated that the reaction proceeded through a bimolecular dehydration mechanism in which water was formed at low temperatures. An intermediate with the stoichiometry of formic anhydride was proposed (*11*), but high-resolution electron energy loss spectroscopy (EELS) studies (*14*) indicated that the intermediate was not an anhydride; it consisted of formate and carbon monoxide species that exhibited attractive interactions. These lateral interactions, which resulted in species that were tightly coupled but not necessarily chemically bonded, were apparently responsible for the autocatalytic decomposition of formic acid on Ni(110) (*14*).

Benziger and Schoofs (*15*) found in a more recent study on Ni(111) that the bimolecular dehydration mechanism only occurred when formic acid was adsorbed as a dimer. The dimer adsorption resulted because formic acid dimers are the main species in the gas phase above the low-temperature sources used to dose the crystals. For adsoprtion of a dimer, Benziger and Schoofs observed autocatalytic decomposition and a CO_2/CO ratio of 0.8. For adsorption of the monomer, however, decomposition was slower and the CO_2/CO ratio was 3.3. The monomer reaction was a simple dehydrogenation to form a formate; the small amount of CO product was due to the water–gas shift reaction and CO_2 dissociation; Auger spectroscopy indicated that more oxygen remained on the surface at the end of the monomer experiment.

The differences between the monomer and dimer reactions under ultrahigh vacuum were used by Benziger and Schoofs to explain why steady-state kinetics at moderate pressures did not show agreement with

[1] To whom correspondence should be addressed.

0021-9517/87 $3.00

previous ultrahigh-vacuum studies. A more direct comparison between reaction in ultrahigh vacuum (UHV) on single crystals and reaction at atmospheric pressure on *supported nickel* can be made by carrying out on supported nickel the same TPD experiments that were done under UHV. This is the purpose of this paper. By using deuterated formic acid, the reaction pathways of the individual hydrogens can be followed to determine if a bimolecular dehydration occurs on supported nickel at high pressures. By exposing the supported nickel to formic acid vapor that is in equilibrium with the liquid at room temperature, mostly dimers should be adsorbed on the surface (*15*).

The use of TPD on single crystal nickel, combined with deuterated formic acid (DCOOH), allowed the bimolecular reaction pathway to be detected. The two distinct hydrogen atoms in formic acid followed separate reaction pathways with acid hydrogens reacting to form water during room temperature adsorption, and the carbon-bound hydrogens reacting to form molecular hydrogen at higher temperatures. The water desorbed below room temperature (*12*) to leave an intermediate with an anhydride stoichiometry. When the temperature was raised, the intermediate decomposed to form carbon dioxide and hydrogen simultaneously. Carbon monoxide also formed but remained adsorbed on the surface until higher temperatures.

Thus, the reaction pathway on single crystal nickel for adsorption of formic acid dimer was (*14*):

$$2DCOOH \rightarrow (DCO + DCOO)_a + H_2O(g) \quad (1)$$

$$(DCO + DCOO)_a \rightarrow (CO + DCOO + D)_a. \quad (2)$$

The species in parentheses are bound together by attractive interactions, though the role of the deuterium atom is unclear (*14*). If the deuterium atom was not interacting with the other surface species, then it should have desorbed well before CO_2 formed; instead, it formed D_2 in the gas phase at the same temperature that CO_2 appeared. Decomposition of these adsorbed species then occurred as

$$(CO + DCOO + D)_a \rightarrow D_2(g) + CO_2(g) + CO_a \quad (3)$$

and at higher temperatures, gas phase CO formed,

$$CO_a \rightarrow CO(g). \quad (4)$$

Our studies for DCOOH adsorption on several Ni/SiO_2 catalysts show that indeed the same reaction pathways are followed as seen on single crystal nickel. A number of secondary processes somewhat modify the final spectra, as will be shown. Overall, the agreement between the single crystal and supported catalyst studies is excellent.

EXPERIMENTAL METHODS

A temperature-programmed desorption system similar to that previously described was used (*16*). A 100-mg sample of catalyst was supported on a frit in a quartz reactor, and an inert carrier gas at atmospheric pressure flowed over the catalyst. Immediately downstream, the gas was analyzed with a UTI quadrupole mass spectrometer located in a turbopumped ultrahigh-vacuum system. A microcomputer system simultaneously recorded amplitudes of five mass peaks and the thermocouple voltage. A 0.25-mm-diameter, shielded thermocouple was located in the catalyst bed to measure the temperature. The thermocouple was connected to a derivative-proportional temperature programmer which controlled an electric furnace to provide a constant heating rate of 1 K/s.

A helium carrier gas was used when detecting D_2O, H_2O, and HDO products, and an argon carrier was used to detect D_2 and HD. Separate carrier gases were used because D_2 could not be separated from the mass 4 signal of He, and D_2O could not be separated from the mass 20 signal due to

Ar^{2+}. Carbon dioxide and carbon monoxide products were observed in both carrier gases, and the change in carrier gas had no effect on the CO_2 and CO spectra. The carrier gas flow rates were 200 cm^3/min. The argon carrier was also used for hydrogen adsorption and desorption, and helium was used for CO adsorption and desorption.

All adsorptions were carried out at room temperature. Gases were injected with a pulse valve until saturation was observed, and liquids were injected with a liquid syringe. Water and formic acid were injected slowly (10 min) so that liquid accumulated on the tip of the syringe and then evaporated into the gas phase at close to room temperature; liquid never contacted the catalyst. To obtain reproducible TPD results, 5 μl of formic acid was exposed to the catalyst and data were taken after a 15-min delay for equilibration. An accurate measurement of the amount of formic acid adsorption was difficult since reproducible liquid injections were not possible. Thus, the mass balances have errors of $\pm 15\%$. Separate calibrations were done in He and in Ar by injecting gases with a gas-tight syringe into the carrier gas. A liquid syringe was used for H_2O and D_2O calibrations. Calibrations for HD and HDO were estimated by linear interpolations between H_2 and D_2 and between H_2O and D_2O calibrations, respectively. Little exchange occurred when D_2O was injected, but the stainless-steel tubing between the reactor and the mass spectrometer was maintained at 360 K to minimize water adsorption on the walls.

Corrections were made for the contribution to the mass 28 signal from CO_2 cracking in the mass spectrometer and to the mass 18 signal from both formic acid and D_2O cracking.

Materials

The 15.6% Ni/SiO_2 catalyst used for most of the studies was prepared by impregnation of nickel nitrate on Davison 57 grade silica (*17*). A 2% Ni/SiO_2 catalyst prepared by impregnation gave similar results. After catalyst preparation (final reduction temperature was 773 K), oxygen in helium was used to passivate the nickel. Before TPD, the catalysts were pretreated in hydrogen for 2 h at 773 K. Nickel loadings were measured by atomic absorption.

Formic-*d* acid (DCOOH) was obtained from MSD Isotopes and was 98.6% deuterated according to NMR analysis. A small water impurity may be present since the freezing point was below 0°C. The D_2O (99%) was obtained from MSD Isotopes. Distilled H_2O and D_2 (99.7%, U.S. Services, Inc.) were used without further purification.

The helium carrier gas was purified by flow through a Matheson Deox unit and then through a molecular sieve trap cooled to liquid nitrogen temperatures. The argon was purified by a molecular sieve cooled in an ethanol slush. Hydrogen was purified with an Engelhard deoxo catalyst followed by a liquid-nitrogen-cooled, molecular sieve trap. The carbon monoxide was purified by flow through activated carbon in an ethanol slurry bath.

RESULTS

A silica support was used for the nickel catalysts since much less formic acid adsorbs on silica (less than 10 μmol/g) than a nickel/silica catalyst (210 μmol/g). Another reason for using silica is that it does not adsorb large quantities of CO, H_2, or CO_2 (*19*). Water is also adsorbed less strongly on SiO_2 than on other supports such as Al_2O_3 (*19*). Thus the rate that products appear in the gas phase are less strongly influenced by readsorption on and subsequent desorption from the SiO_2 support than from other supports. Decomposition of formic acid was also studied on nickel/alumina catalysts (*20*), but the alumina adsorbed large quantities of formic acid, water, and carbon dioxide.

Temperature-programmed decomposition of formic acid on baked silica (heated at 873 K for 24 h) yielded mostly carbon

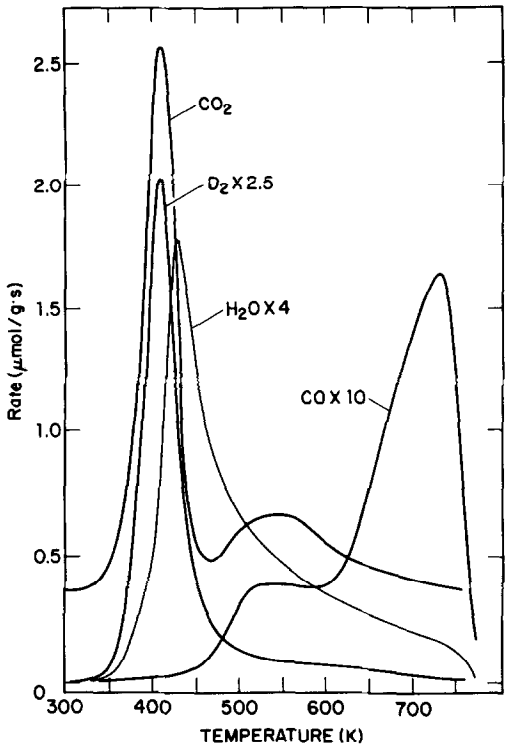

FIG. 1. Temperature-programmed decomposition spectra of the major products from DCOOH decomposition on 15.6% Ni/SiO$_2$. The CO_2 curve is displaced vertically for clarity. Scale factors indicate that the signal was multiplied by the indicated numbers to place them on the y-axis.

dioxide and hydrogen in a 1 : 1 ratio; a quarter of the adsorbed formic acid desorbed unreacted. Silica was not a good catalyst for formic acid decomposition; the reaction products were only observed above 600 K (*20*), and thus they did not interfere with observation of decomposition products from the nickel surfaces. Iglesia and Boudart (*21*) saw somewhat different products from formic acid decomposition on silica, though a similar low activity was observed. They saw both CO and CO_2 at 575 K and the amount of products was similar to the amount from the copper in their copper/silica catalysts. The differences from our study are probably due to the use of a different silica and a different pretreatment. We observed both CO and CO_2 products on silica that was not pretreated at 873 K.

The decomposition of formic acid was carried out on two nickel/silica catalysts that had weight loadings of 15.6 and 2% nickel. The two catalysts yielded similar results; most of the data reported are for the 15.6% catalyst. During programmed heating, almost all of the 210 μmol/g of formic acid that adsorbed on the 15.6% catalyst decomposed. The small amount of unreacted formic acid desorbed with a peak near 375 K. The TPD spectra for the main products from decomposition of DCOOH on nickel/silica are shown in Fig. 1. Carbon dioxide was the largest product and it formed in a relatively narrow peak (40 K halfwidth) with a peak temperature of 412 K. A smaller and broader CO_2 peak was seen at 539 K. At the same temperature as the low temperature CO_2, a narrow D_2 peak was seen. The water product (H_2O) was observed at a somewhat higher temperature and it exhibited a long tail such that desorption was not complete until 773 K. Carbon monoxide formed above 450 K in two broad peaks, and most of the CO was above 650 K. The CO product peak in Fig. 1 was corrected for cracking of carbon dioxide in the mass spectrometer.

In addition to the D_2 and H_2O products, the other isotopes of dihydrogen and water were also seen (Fig. 2). The H_2 and HD peaks had the same peak temperature as D_2 (Table 1), but were slightly broader, and more of the H_2 and HD desorption was in the high-temperature tails. Note, however, that the amount of H_2 was quite small (Table 2) and that the high-temperature tail in Fig. 2 corresponds to a very small amount of product. Similarly, the HDO and D_2O peaks were similar to the H_2O peak, but correspond to much smaller amounts of water (Table 2). Table 3 shows the distribution of the isotopes for the hydrogen-containing products for both nickel/silica catalysts. Most of the deuterium, originally bound to the carbon atom in formic acid, was present in the dihydrogen product, and most of the hydrogen (H), originally present as the acid hydrogen in formic acid, was present in the

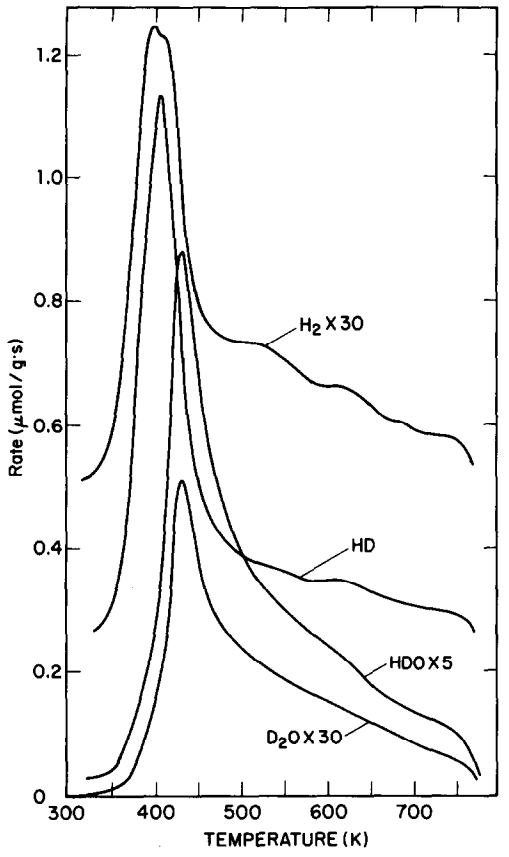

FIG. 2. Temperature-programmed decomposition spectra for the secondary products that contain hydrogen and deuterium from DCOOH decomposition on 15.6% Ni/SiO_2. The curves are displaced vertically for clarity.

water product. For the 15.6% catalyst, 86% of the D was in the dihydrogen products and 63% of the H was in the water products. The HD and HDO products were not present in statistical distributions; only 2% of the deuterium was seen as D_2O and only 4% of the hydrogen was seen as H_2. The temperature-programmed decomposition spectra were similar for the 2% Ni/SiO_2 catalyst, and the distribution of hydrogen isotopes was similar (Table 3).

The CO_2 : CO ratio for the 15.6% Ni/SiO_2 catalyst was 3.8, but this was influenced by disproportionation of adsorbed carbon monoxide, as will be discussed. The mass balances (Table 2) were reasonable considering that data were always obtained in two separate experiments, one in He flow and one in Ar flow. The calibration for water was also difficult. The correction for CO_2 cracking introduced additional error since the large CO_2 peak caused a large correction to the smaller CO peak. Some of the carbon monoxide may have desorbed above 773 K and have not been detected (*19*).

TABLE 1

Peak Temperatures (K) on 15.6% Ni/SiO_2

	Temperature
DCOOH decomposition	
CO_2 (in He)	412, 539
CO_2 (in Ar)	411, 536
CO	535, 731
D_2, HD, H_2	411
H_2O, D_2O, HDO	425
CO adsorption	
CO	450, 700, 775
CO_2	550
H_2 adsorption	
H_2	435

Adsorption of Reaction Products

The reaction products were also separately adsorbed and desorbed from the Ni/

TABLE 2

Product Quantities (μmol/g) on 15.6% Ni/SiO_2

CO_2	152(107)[a]	Total C	192(237)
CO	40(130)	Total H	256
D_2	49	Total D	212
HD	84	Total O/2	219
H_2	5		
H_2O	68		
HDO	26		
D_2O	2		

[a] Numbers in parentheses represent estimates of the amounts of CO_2 and CO initially formed. The disproportionation of CO to form CO_2 and carbon yielded the measured values.

TABLE 3

Distribution (%) of Hydrogen-Containing Products

Product	15.6% Ni/SiO_2	2% Ni/SiO_2
Water		
H_2O	71	81
HDO	27	18
D_2O	2	1
Hydrogen		
H_2	3	8
HD	61	68
D_2	36	24

SiO_2 catalysts. At room temperature, carbon dioxide does not adsorb on clean nickel/silica, though it does adsorb on nickel/alumina (*19*). At elevated temperatures, CO_2 adsorbs by dissociating into CO and O, and the resulting desorption is similar to that seen for carbon monoxide adsorption (*19*). Carbon monoxide desorption was similar to that reported previously; CO desorbed over a wide temperature range with three peaks at 450, 700, and 775 K. It also disproportionated to carbon dioxide with a peak at 550 K. Similar results for TPD of CO were reported by Lee *et al.* (*22*). Hydrogen desorption was similar to that reported by Lee and Schwarz for high-loading Ni/SiO_2 (*23*). It desorbed in a broad peak at 435 K and desorption was seen up to 700 K due to readsorption on the nickel (*24*). Table 1 compares peak temperatures for product desorption (following adsorption of the product) to that for products from formic acid decomposition.

DISCUSSION

Using temperature-programmed decomposition of formic acid on a supported nickel catalyst at atmospheric pressure allows a direct comparison to TPD studies under ultrahigh vacuum on single crystal nickel. Although TPD has been used in numerous studies under UHV, few studies have attempted to make comparisons to these studies by similar TPD studies on supported catalysts. Formic acid decomposition is well suited for such comparisons since it has been extensively studied on several crystal faces and many details on the mechanism appeared to be established. Also, since the decomposition exhibits two pathways, dehydration and dehydrogenation, reaction products for each of the pathways can be followed.

Recent studies by Benziger and Schoofs (*15*) indicate that most of the earlier studies on single crystal nickel under UHV used formic acid adsorbed as a dimer on the surface, due to the exposure of formic acid from a low-pressure, low-temperature source (formic acid solid). For exposure of the same surface to the monomer, different kinetics were observed. In the present experiments, the vapor pressure above formic acid liquid at 300 K was used, since this is the most convenient method to dose the larger quantities needed for high-surface-area catalysts and since this corresponds to the general conditions used for previous kinetic studies on supported nickel. At equilibrium for these conditions, approximately 75% of the partial pressure of formic acid should be due to the dimer (*25*). For equal sticking probabilities of monomer and dimer on the surface, approximately 86% of the formic acid *molecules* on the surface would be from the dimers. Thus, our studies on Ni/SiO_2 should be directly comparable to most of the studies on Ni(110), Ni(100), and Ni(111) surfaces, for which dimers were used.

Comparison of Fig. 1 to data obtained on single crystals shows that indeed many similarities exist between TPD on Ni/SiO_2 and that on single crystal nickel. A one-to-one correspondence is not expected since the higher pressure used for the supported catalysts allows additional secondary reactions that do not occur at the lower pressures used for the single crystals. The support also creates an additional surface for readsorption to occur, as will be discussed.

The similarities imply that the same mechanism is operating under both condi-

tions. Carbon dioxide and deuterium (from the carbon-bonded hydrogen) both form at the same temperature and in a narrow peak. For a supported catalyst, which consists of a distribution of crystal faces and which can also exhibit readsorption at these pressures, the peak widths of 40 K are fairly narrow. Since CO_2 does not adsorb significantly on supported nickel except by dissociating (*19*), the formation of CO_2 is limited by a surface reaction step. Since the D_2 desorption does not correspond to the desorption seen for adsorbed hydrogen, D_2 is also formed by the same reaction-limited step. Thus, a surface intermediate decomposes to form CO_2 and D_2. The decomposition temperatures are somewhat higher on Ni/SiO_2 than on single crystal nickel.

Ten times as much D_2 forms as H_2, and 35 times as much H_2O forms as D_2O, indicating that the two hydrogens in a formic acid molecule follow different pathways, as seen on the single crystals. The acid hydrogens form mostly water and the carbon-bound hydrogens form mostly dihydrogen.

Carbon monoxide is also formed as a product in significant quantities. The carbon monoxide does not form at the same temperature as the CO_2, but is delayed to higher temperatures and CO formation is limited by desorption. This occurs on both supported and unsupported nickel, since a CO adsorption state is available at the temperature that the intermediate decomposes. The CO desorption peaks in Fig. 1 are quite similar to the high-temperature peaks seen for carbon monoxide adsorbed alone on Ni/SiO_2 (*19*).

These results indicate that the mechanism on the supported nickel is similar to that on the single crystal. The dimer reacts, upon adsorption, to form water and an intermediate, $(DCO + DCOO)_a$, which is present perhaps as $(CO + D + DCOO)_a$ and which is stabilized by attractive interactions.

The intermediate decomposes to form D_2 and CO_2 simultaneously in a relatively narrow temperature range:

$$(DCO + DCOO)_a \rightarrow CO_2(g) + 2D(a) + CO(a). \quad (5)$$

The D atoms recombine rapidly to form D_2 at essentially the same temperature that CO_2 forms; the CO remains adsorbed on the surface. Since all the D_2 forms in one peak, it seems unlikely that the two species decompose independently, or two distinct D_2 peaks would be expected. Madix *et al.* (*14*) concluded, however that the decomposition reaction, once started, was so fast that differences in rates of different intermediates could be masked.

Water desorbs at a higher temperature than CO_2 and D_2, but its desorption is probably delayed by adsorption on the support (*26, 27*). On the single crystals, where no adsorption sites are available, the water forms and leaves the surface during the room temperature adsorption.

At higher temperatures on Ni/SiO_2 some of the adsorbed CO disproportionates and the CO_2 that forms rapidly desorbs, with a peak at 539 K.

$$2CO(a) \rightarrow CO_2(g) + C(a). \quad (6)$$

The remaining CO desorbs at higher temperatures,

$$CO(a) \rightarrow CO(g). \quad (7)$$

This CO_2 peak at 539 K is also observed when CO is adsorbed on the surface alone (*19*). This reaction is not observed on the single crystals because of the lower pressures and because CO desorbs from single crystal nickel at lower temperatures, and thus is not present to undergo subsequent reactions.

The presence of CO disproportionation distorts the primary product distributions since some CO that is formed as a primary product is converted to CO_2. The measured CO_2 : CO ratio was 3.8, but an estimate can be made of the initial amounts of CO_2 and CO by measuring the amount of CO_2 in the peak at 539 K. Approximately 45 μmol/g of CO_2 appears to form from CO disproportionation. If this amount is subtracted from

the CO_2 total and 90 μmol/g is added to the CO (to account for the stoichiometry in the disproportionation reaction), then the initial CO_2:CO ratio is approximately 1 (see values in parentheses in Table 2). This agrees with the values of unity that were measured on Ni(110) (*8*) and Ni(100) (*13*).

Thus, the disproportionation of CO appears to be responsible for most of the difference in CO_2:CO ratios for Ni/SiO_2 and single crystal nickel. The water–gas shift reaction could also increase the CO_2:CO ratio, but its effect probably was not large at the carrier gas flow rates used for the data presented. At lower flow rates, a larger CO_2:CO ratio was seen, but the ratio did not increase for flow rates above those used to obtain Fig. 1 (*20*). The fact that some of the formic acid may adsorb as a monomer that decomposes to form mainly CO_2 and H_2 would also increase the ratio (*15*). Subtraction of the CO_2-cracking fraction from the mass 28 signal can also introduce errors that are magnified by taking ratios. On some single crystal surfaces, formic acid has been observed to oxidize the nickel (*15*), though the monomer was observed to leave more oxygen on the surface than the dimer; this could affect the CO_2:CO ratio observed on Ni/SiO_2. Considering the accuracy of the measurements, the overall mass balances are thus quite good, as shown by the total amounts of C, H, D, and O leaving the surface (Table 2). The amount of carbon leaving the surface is low, but this is expected if the disproportionation reaction deposits carbon on the surface. If the estimated amount of deposited carbon from disproportionation is added to the total carbon desorbing, the carbon balance is also good (values in parentheses in Table 2).

The CO_2 and D_2 peaks are broader on Ni/SiO_2 than on single crystal nickel, most likely because of the distribution of surface planes on Ni/SiO_2 and because of readsorption. The possible presence of both dimers and monomers in the gas phase during adsorption can also result in two reactions that appear as one peak over a broader temperature range. The CO_2 and D_2 peaks are still relatively narrow for supported catalysts. On single crystal nickel, peaks were 14–18 K wide on Ni(100) for dimer adsorption (*13*). They were only 5–6 K wide on Ni(110) and 10 K wide on Ni(111). For monomer adsorption on Ni(111), peaks were 22 K wide (*15*). Thus, the halfwidths observed for the supported nickel are quite reasonable.

For room temperature adsorption on single crystal nickel, water is formed from the acid hydrogens as adsorption occurs; the water immediately desorbs. If the same mechanism operates on supported nickel, water also forms as adsorption occurs, but most it remains adsorbed on the silica (*26*). A small amount of unreacted formic acid also desorbs at low temperature, but it corresponds approximately to the amount expected from the support; unreacted formic acid does not appear to be on the nickel after room temperature adsorption. It is likely that some water desorbs from the surface at room temperature and thus the total amount of water measured is lower than that expected for a dehydration reaction. The water calibration is also the least accurate of these measurements because a liquid syringe was used for the calibration. The delay in water desorption to higher temperatures than seen on the single crystal allows time for additional reactions (water–gas shift, exchange of H and D) to occur on the supported catalyst.

A significant fraction of the deuterium is present as HD instead of D_2. The distribution is not statistical, however, and very little H_2 is seen. Under our reaction conditions the exchange reaction

$$D_2 + H_2O \rightarrow HD + HDO \qquad (8)$$

can readily occur on Ni/SiO_2 catalysts (*28*). Because water desorbs from SiO_2 at the same temperature that D_2 forms, the water is available for reaction. This accounts for the HD and HDO and the small amount of D_2O in the products.

Some HD and H_2 may result from de-

composition of the adsorbed monomer. As the monomer decomposes to a formate, hydrogen atoms form and recombine. Hydrogen desorbs from Ni/SiO_2 at a higher temperature than from single crystal Ni so that the H atoms that form at low temperatures are available for reaction with the D atoms that form when the intermediate decomposes. For the monomer, Benziger and Schoofs (*15*) saw that the H_2 from the monomer formed before the formate decomposed, so two distinct peaks were present. In our study, since H_2 desorbs at a higher temperature from Ni/SiO_2, the two peaks would be present at the same temperature.

Thus, the same mechanism appears to be operating on single crystals and on supported catalysts, but the presence of a support that can adsorb products, the different bonding of H_2 to the two surfaces, the distribution of sites on Ni/SiO_2, the higher pressures, the exchange and disproportionation reactions, and the different distributions of dimer and monomer in the two experiments all modify the spectra somewhat.

CONCLUSIONS

Formic acid decomposition on nickel/silica catalysts at atmospheric pressure appears to follow the same reaction pathway as seen for single crystal nickel under ultrahigh vacuum when similar temperature-programmed decomposition experiments are carried out. Adsorbed dimer reacts to form water from the acid hydrogens and leaves a surface intermediate that is composed of a formate and a HCO group, bound together on the surface by attractive interactions. This intermediate decomposes to form carbon dioxide and dihydrogen, which desorb, and adsorbed carbon monoxide, which desorbs from the surface at higher temperatures. The amount of decomposition on the silica support is insignificant, but readsorption of water occurs. The supported catalysts show some differences from the single crystals because of readsorption at the higher pressures used, CO disproportionation, and exchange reactions, and because of the distribution of sites presented on supported nickel.

ACKNOWLEDGMENTS

The authors gratefully acknowledge support of this work by the National Science Foundation under Grant ENG 77-15356 and Equipment Grant CPE 79-23208. We thank Mark A. Strobel and William J. Ruzinsky for carrying out preliminary experiments. We also thank Tracy Rold of IBM for NMR measurements and Kathy Kierein and Phuong Chi Pham for help in data reduction.

REFERENCES

1. Mars, P., Scholten, J. J. F., and Zwietering, P., in "Advances in Catalysis" (D. D. Eley, P. W. Selwood, and P. B. Weisz, Eds.), Vol. 14, p. 35. Academic Press, Orlando, FL, 1963.
2. Bragg, J., Jaeger, H., and Sanders, J., *J. Catal.* **2,** 449 (1963).
3. Duell, J. J. and Robertson, A. J. B., *Trans. Faraday Soc.* **57,** 1416 (1961).
4. Sosnovsky, H., *J. Chem. Phys.* **23,** 1486 (1955).
5. Fukuda, K., Nagashima, S., Noto, Y., Onishi, T., and Tamaru, K., *Trans. Faraday Soc.* **64,** 522 (1968).
6. Sachtler, W. M. H., and Fahrenfort, J., "Actes du Deuxieme Congres Internationale de Catalyse, Paris, 1960," p. 831. Ed. Technip, Paris, 1961.
7. Tamaru, K., *Trans. Faraday Soc.* **55,** 824 (1959).
8. McCarty, J. G., Falconer, J. L., and Madix, R. J., *J. Catal.* **30,** 235 (1973).
9. Falconer, J. L., and Madix, R. J., *Surf. Sci.* **46,** 473 (1974).
10. Falconer, J. L., McCarty, J. G., and Madix, R. J., *Surf. Sci.* **42,** 329 (1974).
11. Madix, R. J., and Falconer, J. L., *Surf. Sci.* **51,** 546 (1975).
12. Falconer, J. L., and Madix, R. J., *J. Catal.* **51,** 47 (1978).
13. Benziger, J. B., and Madix, R. J., *Surf. Sci.* **79,** 394 (1979).
14. Madix, R. J., Gland, J. L., Mitchell, G. E., and Sexton, B. A., *Surf. Sci.* **125,** 481 (1983).
15. Benziger, J. B., and Schoofs, G. R., *J. Phys. Chem.* **88,** 4439 (1984).
16. Falconer, J. L., and Schwarz, J. A., *Catal. Rev. Sci. Eng.* **25,** 141 (1983).
17. Bartholomew, C. H., and Farrauto, R. J., *J. Catal.* **45,** 41 (1976).
18. Ruzinsky, W. J., Master's thesis, University of Colorado, Department of Chemical Engineering, 1980.
19. Falconer, J. L., and Zagli, A. E., *J. Catal.* **62,** 280 (1980).
20. Strobel, M. A., Master's thesis, University of Col-

orado, Department of Chemical Engineering, 1979.
21. Iglesia, E., and Boudart, M., *J. Catal.* **88,** 325 (1984).
22. Lee, P. I., Schwarz, J. A., and Heydweiler, J. C., *Chem. Eng. Sci.* **40,** 509 (1985).
23. Lee, P. I., and Schwarz, J. A., *J. Catal.* **73,** 272 (1982).
24. Falconer, J. L., Bailey, K. M., and Gochis, P. D., *in* "Catalysis of Organic Reactions, Chemical Industries," Vol. 22, p. 135. Dekker, New York, 1985.
25. Coolidge, A. S., *J. Amer. Chem. Soc.* **50,** 2166 (1928).
26. Zagli, E., and Falconer, J. L., *J. Catal.* **69,** 1 (1981).
27. Zagli, A. E., Falconer, J. L., and Keenan, C. A., *J. Catal.* **56,** 453 (1979).
28. Marginean, P., and Olariu, A., *J. Catal.* **95,** 1 (1985).